CONSEIL INTERNATIONAL
DES MACHINES A COMBUSTION

INTERNATIONAL COUNCIL
ON COMBUSTION ENGINES

PAPER NO.: 53
Advanced optical development tools for two-stroke marine diesel engines

Stefan Mayer, MAN Diesel and Turbo, Denmark
Johan Hult, MAN Diesel and Turbo, Denmark
Karl Johan Nogenmyr, MAN Diesel and Turbo, Denmark
Soennik Clausen, Technical University of Denmark, Denmark

Abstract: Development and application of advanced engineering tools - for description, prediction and optimization of the 2-stroke Diesel engine process - is essential for development of the marine engines of the future. Here, recent developments of optical and laser based imaging tools will be presented. Such tools can lead to both increased understanding and predictive capabilities of for example the scavenging process, fuel spray structure, flame ignition, and thermal loads. For optical studies access to the combustion chamber has been achieved using sapphire windows, mounted in starting air and fuel injector ports on both standard fuel oil and gas cylinder covers, or inserted in the 24 optical ports of a dedicated optical cover. A few examples, highlighting the new capabilities thus offered, will be presented. High-speed imaging offered detailed views of the dynamics of fuel jet ignition. Pulsed laser illumination was used for visualization of fuel jets, from which information on fuel jet penetration, jet velocity, and spray angles could be gathered. For this purpose a high-power laser and a custom designed imaging system was mounted directly onto the optical cover. The fuel jet data is qualitatively compared to results from KIVA simulations, in order to tune spray parameters in the numerical model. The same laser system was also used for measurements of in-cylinder flow velocities, in order to characterize swirl and scavenging. Particle image velocimetry (PIV) was used for those velocity measurements. Finally, infrared imaging was employed for two purposes, firstly for capturing the evolution of piston temperature distributions during single engine cycles and secondly for visualization of scavenging of hot product gases.

INTRODUCTION

Just as for the smaller engines refinement of large-bore two-stroke Diesel engines, with reduced pollutant emissions and improved performance, will require improved engine designs. For such a development advanced optical imaging tools are desirable, both for testing new engineering designs and for validating computational models used in such work. At the two-stroke division of MAN Diesel&Turbo in Copenhagen we have built up our capabilities to employ optical and laser based measurements during the last couple of years. Here we will demonstrate some of those capabilities and also illustrate how those now drive the validation of our computational CFD tools for engine simulation.

Optical and laser based diagnostics have been applied extensively on car and truck sized engines, and has led to a more thorough understanding of in-cylinder processes [1-2]. Optical measurement techniques for studying flow fields, fuel injection, ignition, combustion, pollutant formation, lubrication and heat loads have been developed [3-5]. Such measurement techniques can be used as advanced engineering tools during development, to shed light on fundamental processes, or for validation of computational tools.

For the larger marine engines, however, such optical techniques have not yet had the same impact. A number of studies have been reported on medium-speed four-stroke diesel engines, with bore diameters ranging from 200 to 320 mm. These include high-speed photography [6], flame pyrometry [7], and laser Mie scattering for spray studies [8-11]. In those studies either borescopes [6-7,10-11] or windows with the thickness of the engine wall [8-9] were used to obtain optical access to the cylinder interior, thus limiting either collection efficiency or field-of-view. Concurrently, optical and laser based diagnostics has also been applied to constant volume combustion chambers [12-14] and rapid compression machines [15] with sizes relevant for low-speed marine engines. In such systems excellent optical access can be obtained, and data on sprays, ignition and combustion can be acquired during reasonably engine relevant conditions.

Optical diagnostics in full size marine engines pose a number of challenges for optical diagnostics, though their size, vibrations, high in-cylinder pressures and thermal loads, intensely sooting combustion, and strict safety requirements. Here we present a modified optical engine cover for a fully operational 500 mm diameter two-stroke engine, with associated optical hardware designed for laser illumination and imaging. The engine cover features 24 optical ports from the side and the top in order to allow optical access to most of the cylinder around top dead centre (TDC). Through positioning of optical elements deep inside the optical ports both wide-angle illumination and efficient signal detection can be achieved. All optical hardware is mounted directly onto the engine – in order to avoid drifts in alignment caused by vibrations or thermal expansion. The performance of this optical engine and imaging system is illustrated here through studies of fuel jet structure, flame ignition, in-cylinder flow field, thermal loads and the scavenging process.

We also present the first steps taken towards validation of numerical tools, based on the data acquired. Fuel jet data measured under different engine operating conditions is qualitatively compared to results from KIVA simulations in order to guide the choice of spray parameters in the numerical model. Velocity data recorded in the vicinity of the exhaust valve is also compared to the results of cycle simulations of flow through the exhaust valve.

EXPERIMENTAL ARRANGEMENTS

Engine

The MAN Diesel&Turbo 4T50ME-X test engine is a production sized turbocharged uniflow scavenged two-stroke Diesel engine, fully equipped for extensive testing. The main characteristic data of the 4T50ME-X engine are summarized in table 1.

Table 1 - Engine specifications.

Engine type	2-stroke Diesel
Cylinders	4
Bore	500 mm
Stroke	2.20 m
Power	7 MW
Max speed	123 rpm
Max pressure	190 bar

Optical access

Individual smaller windows have to be employed for optical access to the interior of the combustion chamber, due to the sheer dimensions of the present engine. In the past we have employed existing ports in the cover, such as the starting air valve or a fuel injector port, for obtaining optical access through the use of inserts fitted with sapphire windows [16]. The starting air valve was used for the IR-imaging reported here. For the laser based diagnostics, however, a larger flexibility is

required and thus a new optical cover was designed. It features 24 ports: 14 from the side (1-14) and 10 from the top (15-24), see Figure 1.

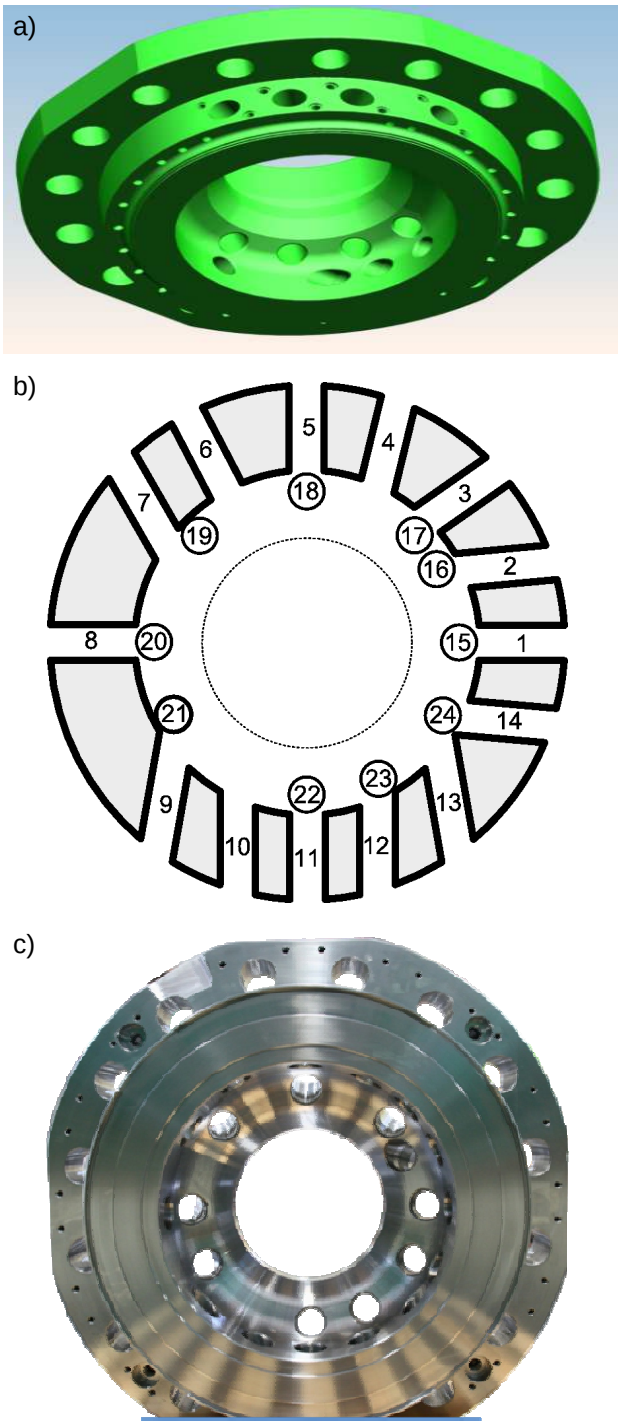

Figure 1 - (a) Illustration of optical cover, (b) schematic overview of port positions, (c) photo of optical cover.

Each port can be used as either an optical port or fitted with a fuel injector, which leads to a large degree of flexibility in the relative positioning of optical instrumentation and fuel injectors. Unused ports are sealed with metal inserts. The entire cover can be rotated in 90° steps with respect to the engine to allow external access to all ports. The holes have a diameter of around 60 mm, and a depth of 125 mm to 140 mm. The holes are distributed unevenly and are not all oriented in the radial direction, to allow various imaging scenarios to be realized. The cover is fitted with internal water cooling in a similar manner to a standard cover. It is designed to allow full load operation, however, only at an overall limited lifetime.

Inserts fitted with sapphire windows at the front are mounted into the ports used for optical diagnostics. Sapphire was chosen as it has acceptable transmission from the UV to the IR, good high-temperature performance, and allows thinner windows to be used compared to quartz due to its higher mechanical strength. The optical clear diameter of a mounted window becomes 40 mm, determined by the inner diameter of the insert tube. Optical elements or modules can be mounted inside those inserts, and be brought to within a millimetre of the window. By employing tight control over engine start-up, operation, and lubrication procedures the optical windows could be kept reasonably clear for up to several hours operation, eventually becoming limited by deposits from combustion and lubrication.

The measured cylinder pressure for the cylinder fitted with the optical cover is shown in Figure 2. The engine was operated at 25% load for this case, as for the PIV measurements presented later. The calculated heat release rate is also plotted.

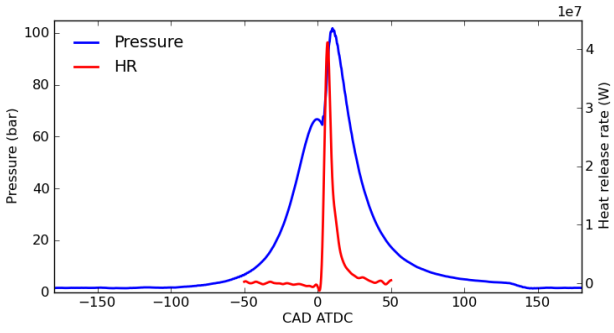

Figure 2 – Cylinder pressure and calculated heat release rate for the cylinder with the optical cover, operated at 25% load.

Performing experiments on a full sized engine, rather than in a combustion or spray cell, leads to increased experimental complexity and unavoidable practical restrictions. Nevertheless, there are several advantages with performing experiments on an actual engine. First of all, realistic conditions are fulfilled by default, e.g. geometry, swirl, thermodynamic state of charge, and thermal

boundary conditions. Secondly, one or several measurements can be performed in each engine cycle, depending on laser repetition rate and camera read-out rate, which leads to favourable overall data rate where statistically significant data sets can be acquired in a relatively short time. For example 100 PIV measurements at 25% load can be performed in just 77 seconds. Furthermore, cycle-to-cycle variations of in-cylinder processes can be estimated, and their effect on overall performance elucidated. Finally, the optical imaging techniques can be used also as an engineering tool for real-time monitoring of the effects of for example tuning injection or valve timings, atomizer layouts, or fuel properties.

Optical mounting

All optical equipment, including cameras and the laser, were mounted directly to the cylinder cover. By mounting all optics to the engine effects of vibrations and thermal drifts on optical alignment can be reduced. This requires the use of highly ruggedized equipment capable of withstanding the rather violent engine vibrations. A photo of the equipment employed for fuel jet visualization mounted on the engine is shown in Figure 3. The laser is seen to the upper right, and the two CCD cameras to the front.

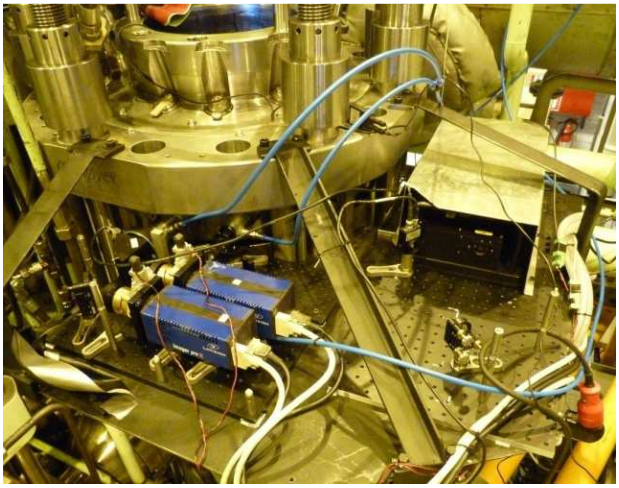

Figure 3 - Photo of laser and cameras mounted on T50ME-X.

FUEL JET PROPAGATION AND IGNITION

Experimental set-up

The experimental arrangement for simultaneous fuel jet and flame emission imaging is illustrated in Figure 4. The various fuel injectors tested were mounted from top-port 17. The fuel jets were illuminated by a divergent laser cone from behind, at a glancing angle, from port 2. The light scattered from the liquid jet and droplets was then detected at approximately right angles from port 12.

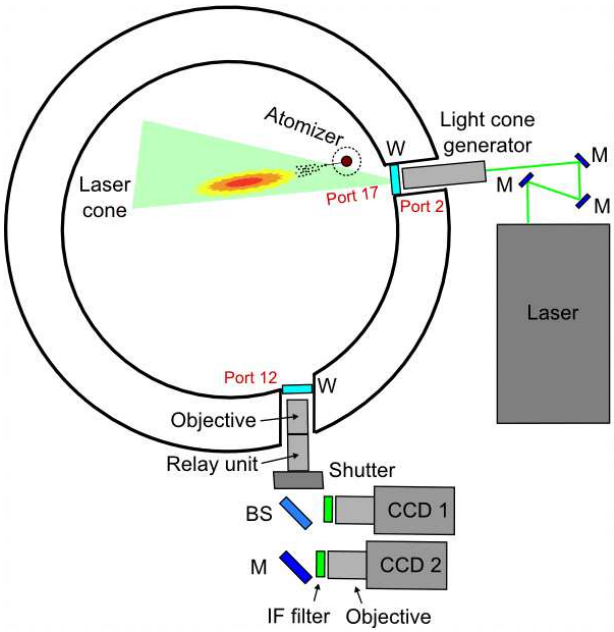

Figure 4 - Schematic outline of experimental arrangement for fuel jet imaging (M: mirror, W: window, BS: beam splitter).

For illumination a ruggedized dual cavity pulsed Nd:YAG laser was used, featuring a pulse length of around 8 ns. The maximum pulse energy at 532 nm was around 200 mJ. In Figure 4 the illumination arrangement is shown. A number of mirrors were used for redirecting the beam into the optical port. A combination of three negative spherical lenses was used to generate a light cone with a half-angle of around 25°. Two wedge prisms were used as the final elements, in order to direct the light cone at an angle of around 20° to the optical axis, in the direction of the fuel nozzle. The illumination optics were all mounted into a lens tube, which was then inserted into the optical insert in port 2 and brought to within a few mm from the sapphire window.

A dual camera system was used for recording both scattered laser light and native flame emission. Two

CCD cameras (2048×2048 pixels, 14 bits) were used, coupled to a common imaging system via a 50% beam splitter. A custom made relay imaging system, with a 50° viewing angle objective at the front, which fits inside the optical ports was used. A mechanical shutter was built into the system in order to discriminate against the strong flame emission. Each camera was fitted with an interference filter, either 1 nm wide centred at the laser wavelength for capturing the laser Mie scattered signal form the fuel jet, or 200 nm wide centred around 500 nm for capturing flame emission. For the Mie scattering shutter times of 1 μs were used, and for the flame emission 15-30 μs. There was a delay of 10 μs between the exposures of the two cameras.

For a first set of experiments, however, a single high-speed camera was used for observing the flame emission during ignition. For this purpose the camera was coupled to the same custom designed imaging optics, but for this purpose a different combination of imaging (4) and atomizer (22) ports was employed, offering a slightly different view.

Experimental results

A high-speed movie of the ignition of a fuel jet, coming from a single-hole atomizer, is shown in Figure 5. The high-speed camera is sensitive in the visible spectral region, and the light observed thus corresponds to black-body emission from hot flame generated soot. This movie has a frame separation of 56 μs (0.025 CAD). One can see that the fuel jet appears to ignite on the top surface, where faint light is seen already in the first frame. This then develops to a thin flame with increasing luminosity on the top of the jet, which then eventually spreads around the jet, both to the bottom side and downstream. At the end a fully developed flame can be seen, which will then propagate further downstream and spread through the cylinder (out of view).

High-speed photography has proved to be a useful engineering tool. At MAN Diesel&Turbo it has been used for investigations of ignition, flame propagation and flame structure within development projects such as gas (ME-GI), exhaust gas recirculation (EGR) and water in fuel (WIF). High-speed imaging, using borescope access through existing holes, has thus already become a routine tool [16].

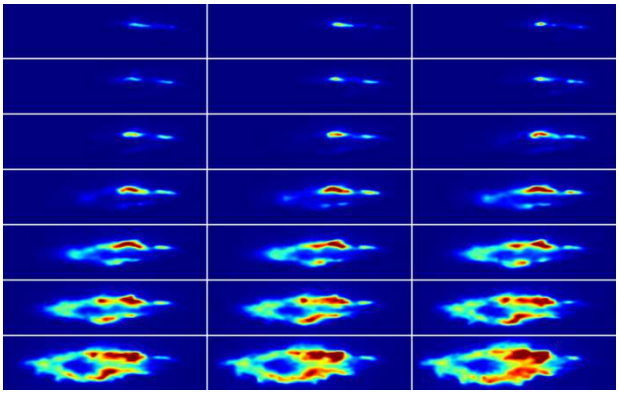

Figure 5 - High-speed sequence of flame ignition for a single-hole atomizer recorded at 18000 frames per second. The first frame corresponds to 4.387 CAD ATDC and the last to 4.912 CAD ATDC, the frame spacing is 0.025 CAD. Field of view: 270×70 mm.

A sequence of simultaneously measured fuel spray and flame emission images are shown in Figure 6. In the left column the Mie scattering from the laser illuminated fuel jet, captured on CCD1, is shown. It marks liquid fuel jet and droplets, and thus illustrates the liquid penetration length. The simultaneously measured flame emission captured on CCD 2 (without laser illumination) is shown in the right column. The images corresponding to different CAD are captured in different cycles, but are plotted as a sequence here to illustrate the injection evolution. In this example the fuel jet is seen to first exit the atomizer at 3.7 CAD ATDC, and then rapidly propagates until 4.3 CAD, at which time the fuel jet ignites on both sides, about half way up the jet. The flame then spreads downstream and evolves into a full flame at a stable lift-off length. The fuel jet appears to retract to a stable length after 4.7 CAD. This retraction could be due to increased rates of evaporation after onset of combustion, or an artefact due to partial obscuration by the soot cloud – and further analysis will be required to settle the issue. At around 10 CAD the injection ends. The Mie scattering signal then quickly diminishes and the flame advances towards the nozzle – before blowing off.

The laser Mie scattering technique can also be used to investigate the difference in fuel jet structure for different types of fuel. In Figure 7 an example is shown, where Diesel and heavy fuel oil (HFO) is injected from the same single-hole injector during identical conditions. One can directly observe several differences. The HFO jet seems to have a slightly larger spray angle, it breaks up into separate islands more quickly, and propagates further.

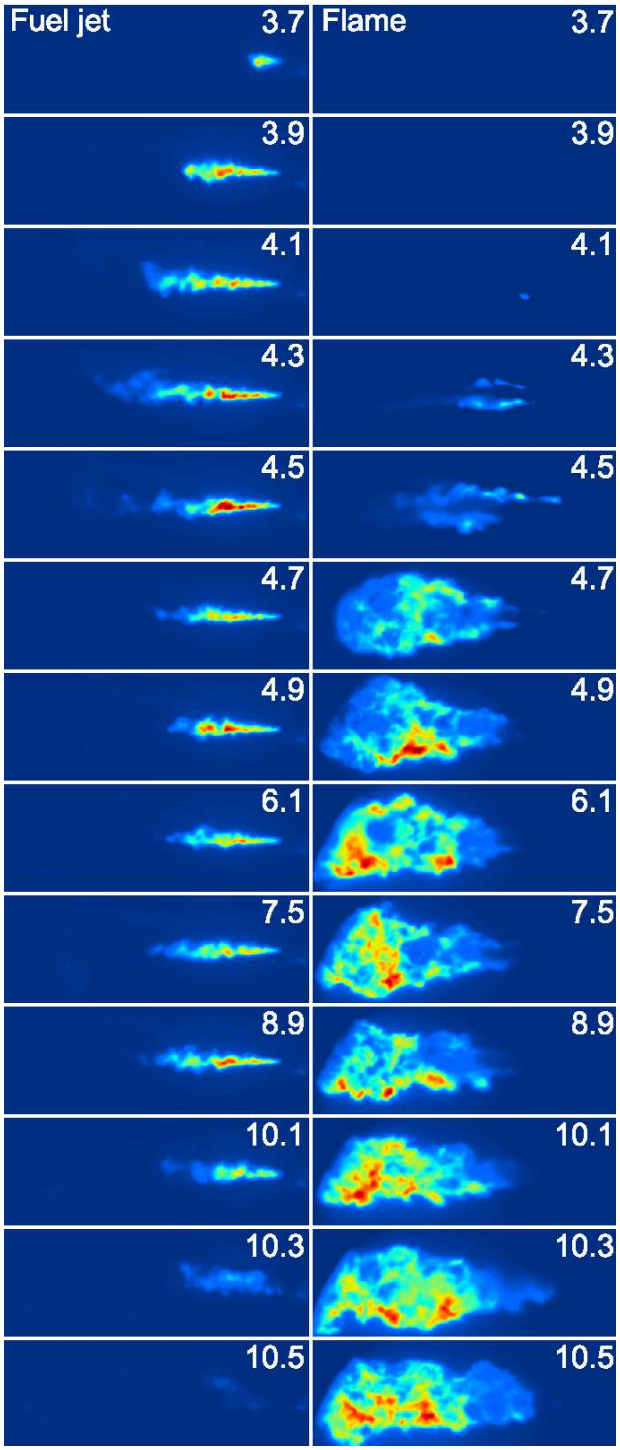

Figure 6 - Simultaneously measured image pairs of Mie scattering (fuel jet) and flame emission from a single-hole atomizer operating on Diesel fuel. Field of view: 196×69 mm, numbers indicate CAD ATDC.

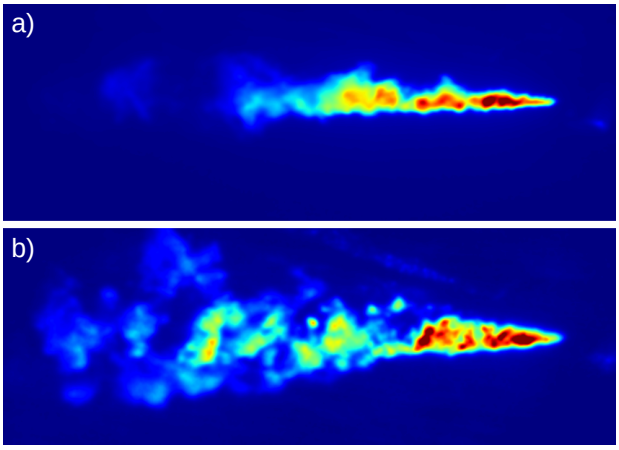

Figure 7 - Single shot Mie scattering images of fuel jet structure: a) Diesel oil, b) HFO. Field of view: 196×69 mm, timing corresponds to approximate time of ignition.

From the Mie scattering images properties like spray angle and liquid penetration length can be extracted, as illustrated in Figure 8. First the image is segmented, as outlined by the solid white line. Penetration length S and spray angle θ are then calculated from the segmented image following the approach of Naber and Siebers [17]. The penetration distance, illustrated by the position of the $\theta/2$ arc terminating the jet centre line, is defined as the distance to the location where 50% of the pixels on an arc of $\theta/2$ are fuel pixels. The spray angle is then defined as the arctangent of the projected fuel jet area of the first upstream half of the jet divided by the square of half the penetration distance. The spray angle is illustrated by the dashed lines.

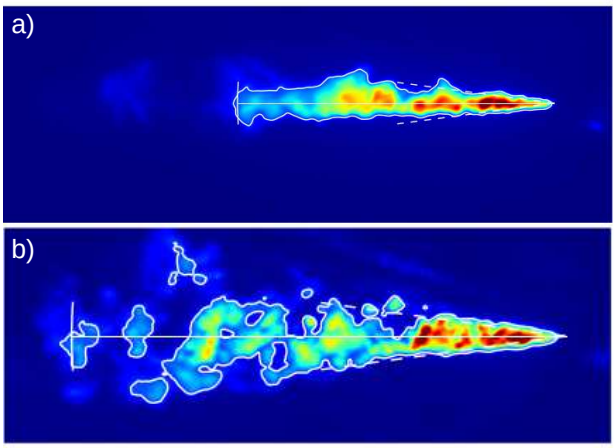

Figure 8 – Segmented fuel jet images, a) Diesel oil, b) HFO. The penetration lengths and spray angles are indicated by the white lines (a: 102 mm & 15.0°, b: 160 mm & 15.6°).

By firing the second laser as well, and changing the IF filter of CCD 2 to a 532 nm interference filter, an image pair of the fuel jet can be acquired during a single injection event, see Figure 9. From such image pairs the fuel jet front propagation velocity can be evaluated. In this example the velocity is seen to drop from around 130 m/s when the fuel first exits the nozzle, to around 60 m/s close to the time of ignition.

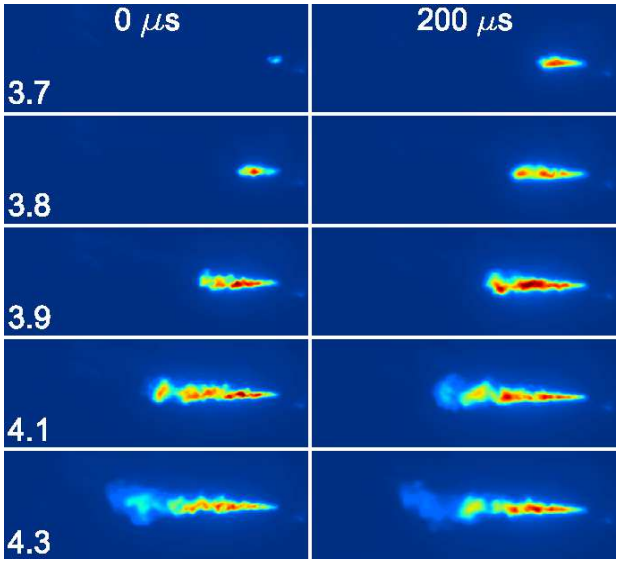

Figure 9 - Double shot (Δt=200 μs) Mie scattering images of fuel jet propagation from a single-hole atomizer. Approximate jet front velocities are 130 m/s, 115 m/s, 77 m/s, 72 m/s, and 59 m/s. Field of view: 196×69 mm, numbers indicate CAD ATDC.

A correct prediction of fuel jet and spray development and structure, as well as of ignition location and development is important for detailed CFD calculations of the combustion process. Data of the type presented here can thus be used as a means of refining those calculations, and thus ultimately improve their predictive capability. For this purpose we have started the work of building up a data base covering a range of engine operating conditions, nozzle layouts and fuels. Properties which can be extracted from the type of data illustrated here includes: spray angle, liquid penetration length, fuel jet velocity, flame lift-off length, ignition timing, and ignition location. For all of those average values as well as statistics of variations can be evaluated.

Comparison to numerical simulations

An example of how the measured fuel jet data can be used for validation of numerical tools will be demonstrated here. Modelling of spray, ignition, combustion and emission formation has been carried out using the KivaMBD CFD code that is based on KIVA 3V2 [18] and sub models originally developed at the Energy Research Centre (University of Wisconsin) [19, 20]. The code has been adjusted and extended in-house by MAN Diesel&Turbo to be valid at the larger length and time scales of marine Diesel engines. Additionally, the fuel aspect has been addressed as well as the accuracy of the thermodynamic description of the cylinder charge gas, which has to be higher for larger engines. KivaMBD has become established as an in-house tool for detailed three-dimensional CFD studies of the working stroke of two-stroke Diesel engines. The code is adapted to the relevant engines at MAN Diesel&Turbo and integrated into a user environment streamlining the work flow. The boundary conditions for the simulations were based

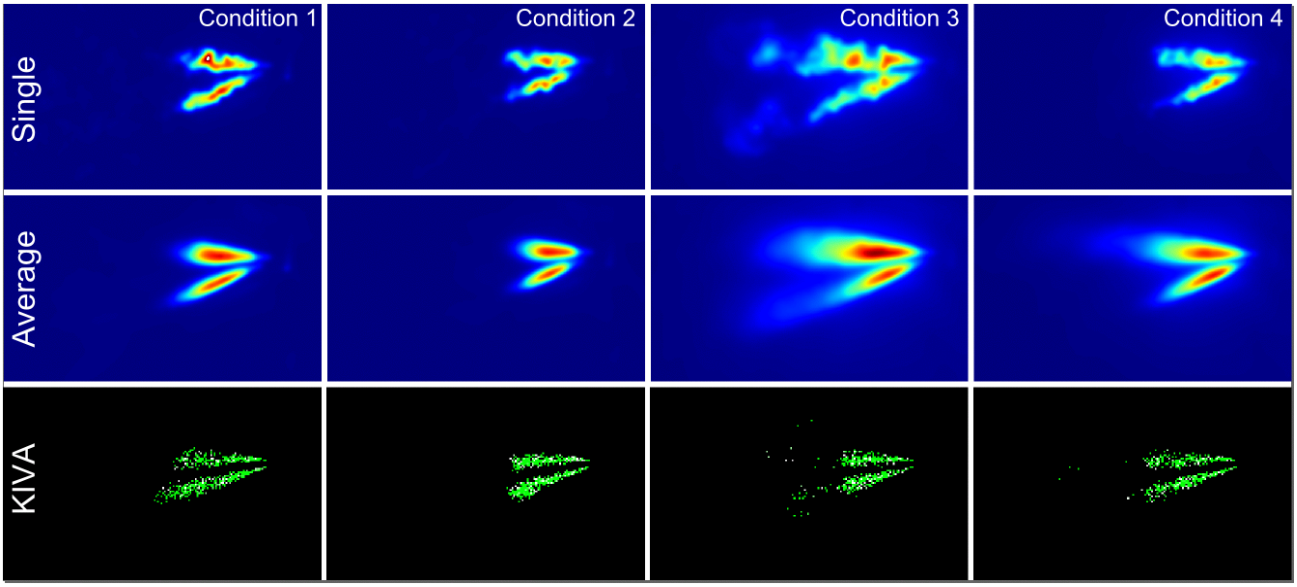

Figure 10 - Top row: single shot images of fuel jets from a dual-hole atomizer operated under four different conditions, second row: averages of 100 images, bottom row: fuel jets predicted using KIVA for corresponding conditions.

on an analysis of measurement data.
An example of how measured and numerical results can be compared is shown in Figure 10. The fuel jets from a dual-hole atomizer are shown, for four different operating conditions (load, scavenge pressure, compression pressure). For example the charge density was about 40% higher in condition 2 compared to condition 1. In the top row examples of single shot images are shown, in the second row the averages over 100 cycles are shown. KIVA simulations were performed for the same operating conditions, while varying spray model parameters. As the physical scale and view is the same for both experiments and simulation a direct comparison can be made, and the choice of parameter leading to the best match could be identified. In the bottom row the calculated spray patterns corresponding to the parameters, giving the best match for all four conditions, are shown.

IN-CYLINDER FLOW

Experimental set-up

Flow velocities can be performed using PIV, through illuminating micrometer sized particles seeded to the flow, with a laser sheet twice – with a short time separation. The light scattered from the particles is then imaged onto a double frame camera. From the particle displacement between the two images the velocity field can be calculated using a cross-correlation technique [21]. For the PIV velocity measurements the laser and camera system was used in a different configuration, see Figure 11. A light sheet generator comprising one spherical lens, three cylindrical lenses and a wedge plate was used to generate a focused laser sheet with diverging height [22]. The sheet was perpendicular to the observation direction, and located around 55 mm from the wall. In this way the velocity components along the circumference (x) and along the height (y) of the cylinder could be measured, thus providing information both on the swirl and on the scavenging. A single CCD camera, operated in double frame mode, was used for the PIV measurement. The field of view was around 50×50 mm. A commercial software (DaVis) was used for PIV data evaluation.

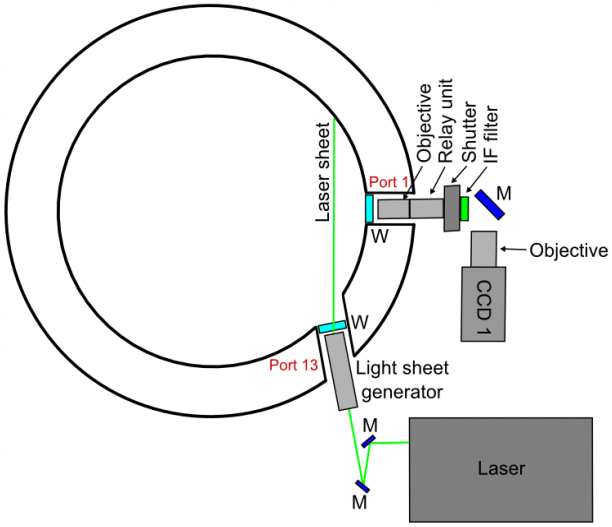

Figure 11 - Schematic outline of experimental arrangement for PIV (M: mirror, W: window).

For the PIV measurements the air flow into the cylinder was seeded with 2.5 µm diameter ZrO particles. A rotary brush seeder was employed to disperse the particles into the scavenging box of the optical cylinder.

Experimental results

An example of a Mie scattering image of the laser illuminated particles is seen in Figure 12. The seeding density and homogeneity is quite good, and particles remained through the entire engine cycle, albeit at lower density and visibility in the expansion stroke. Velocity measurements could thus be performed during the entire cycle, except during combustion when the flame background emission and laser scattering from soot clouds exceeds the Mie scattering signal from the ZrO particles.

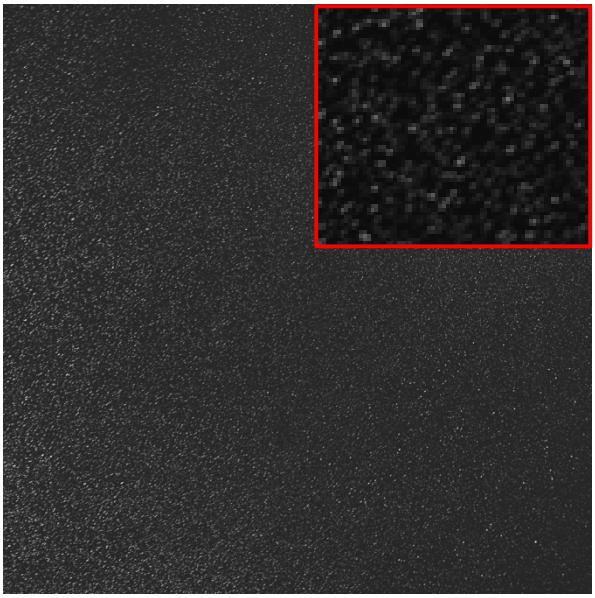

Figure 12 - Example of PIV image of Mie scattering from 2.5 μm diameter ZrO seeding particles, recorded at 270 CAD ATDC. Field of view: 50×50 mm. Insert: magnified view.

The velocity field calculated from the particle image shown in Figure 12 and its associated second frame, recorded 30 μs later, is shown in Figure 13. At this time (270 CAD ATDC) the exhaust valve has just closed and the velocity field exhibits fine structure, with a maximum velocity of around 12 m/s. For the example displayed here interrogation regions of 32×32 pixels, corresponding to 0.8×0.8 mm, were used in the analysis. At this resolution the scale of turbulent structures can be estimated.

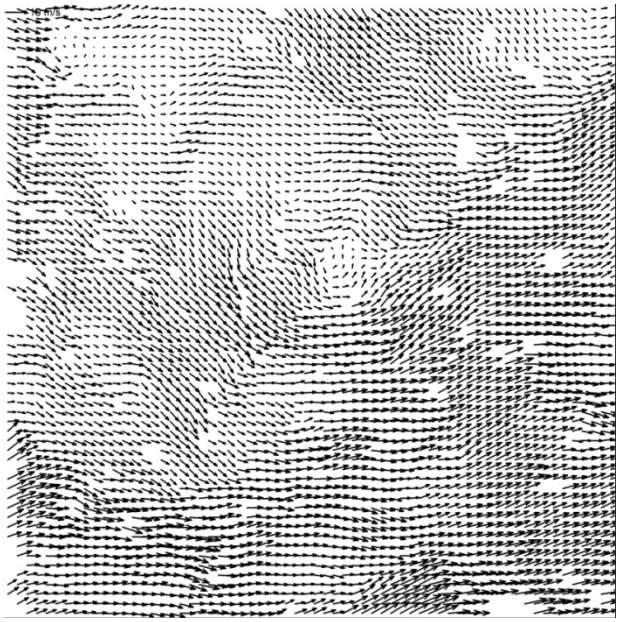

Figure 13 - Velocity field recorded at 270 CAD ATDC. Interrogation regions of 32×32 pixels were employed, resulting in a spatial resolution of around 0.8 mm.

For every 10 CAD a number of frame pairs were recorded in consecutive cycles (10-100, with the largest number of samples in the compression stroke), in order for average velocity fields to be measured. In Figure 14 average velocity fields at four different times in the engine cycle are plotted. For clarity the data has been spatially averaged to a coarser grid (by a factor of four). It is clear that the average velocity over the limited field of view (50×50 mm) is quite homogeneous, and an average velocity over the field of view can be calculated. The x- and y-components of this average velocity are plotted as a function of CAD in Figure 15 a).

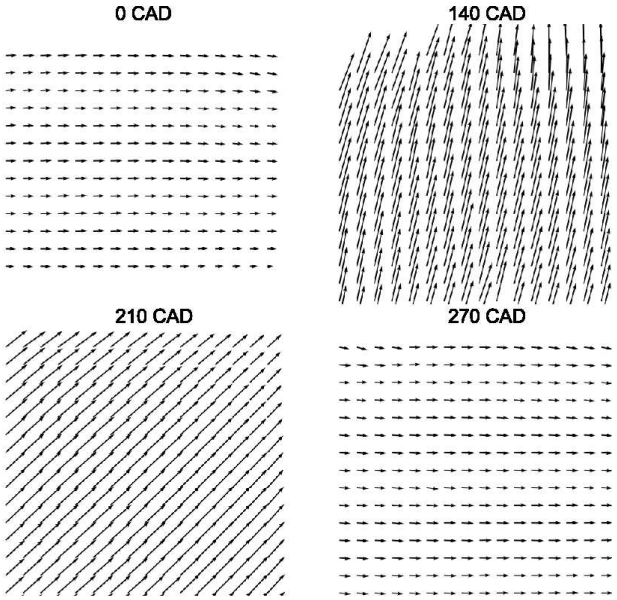

Figure 14 - Average velocity fields measured at four different CAD. Field of view: 50×50 mm, measurement plane located 55 mm from cylinder wall, between top piston and lowest exhaust valve position.

At the location probed the local velocity is driven by the flow out of the exhaust valve when it is open, for this reason a cycle simulation of the average velocity through the exhaust valve is also shown for comparison in Figure 15 b).

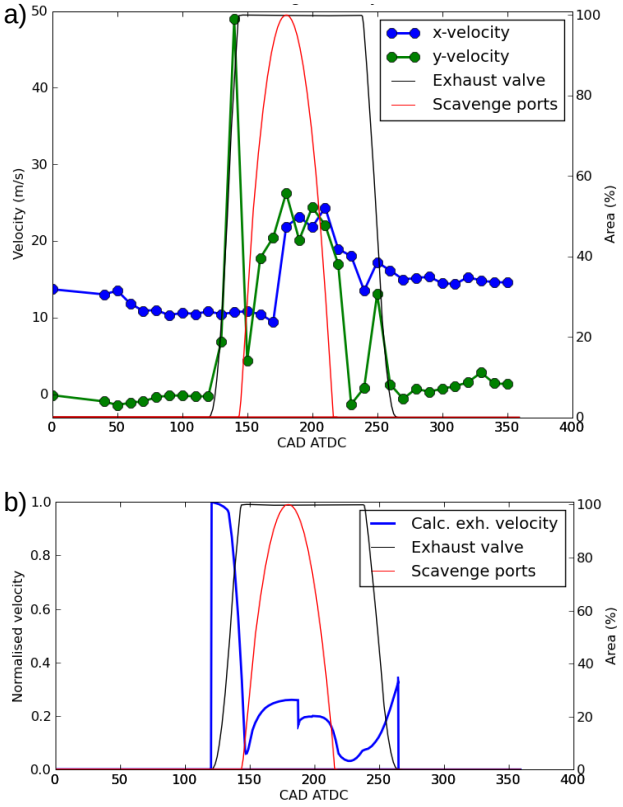

Figure 15 - a) Average velocity fields measured throughout the engine cycle. Measurement location located 55 mm from cylinder wall, between top piston and lowest exhaust valve position. Exhaust valve and scavenge port areas are also plotted. b) Calculated average velocity through exhaust valve.

In this example the x-component (swirl direction) rises at about 30 CAD after the uncovering of the scavenge ports. It then remains at a value around 20-25 m/s during the time they are open. After this it slowly decays during the cycle, from 16 m/s down to 10 m/s just before the scavenge ports are uncovered again.

The y-velocity is close to zero when the exhaust valve is closed. When the exhaust valve opens, it rapidly increases up to 50 m/s as the burnt gases are pressed out by the over pressure in the cylinder. It then dips shortly before the scavenging starts to drive the flow out again, at a velocity of around 20 m/s, until the scavenge ports close. There is then a final small peak just before the exhaust valve closes, as the gases are staring to be pressed out through the compression. The measured y-velocity qualitatively compares quite well to the calculated flow through the exhaust valve, shown in Figure 15 b).

IR IMAGING

Experimental set-up

For the IR-imaging the starting air valve on a standard cover was employed, see Figure 16. A fast IR-camera with 1.5-5.1µm spectral response was used. It was coupled to a specially designed wide-angle IR-endoscope, via a mirror, to look downwards in the cylinder to obtain a stable setup for thermal imaging of the piston. A number of different optical filters were mounted in the internal remote-controlled filter wheel of the IR-camera. Firstly, a 3900 nm optical filter was used for measurements of piston surface temperature, as the thermal emission from gas bands is very low in this region. Secondly, a 4525 nm optical filter was used for visualising hot gases during scavenging, as CO_2 has a so called “hot-band” in this spectral region. The optics were sufficiently efficient to give images with low noise and sufficient time resolution to follow temporal behaviour of the piston surface temperatures or to visualize gas flow patterns based on thermal radiation emitted from hot CO_2.

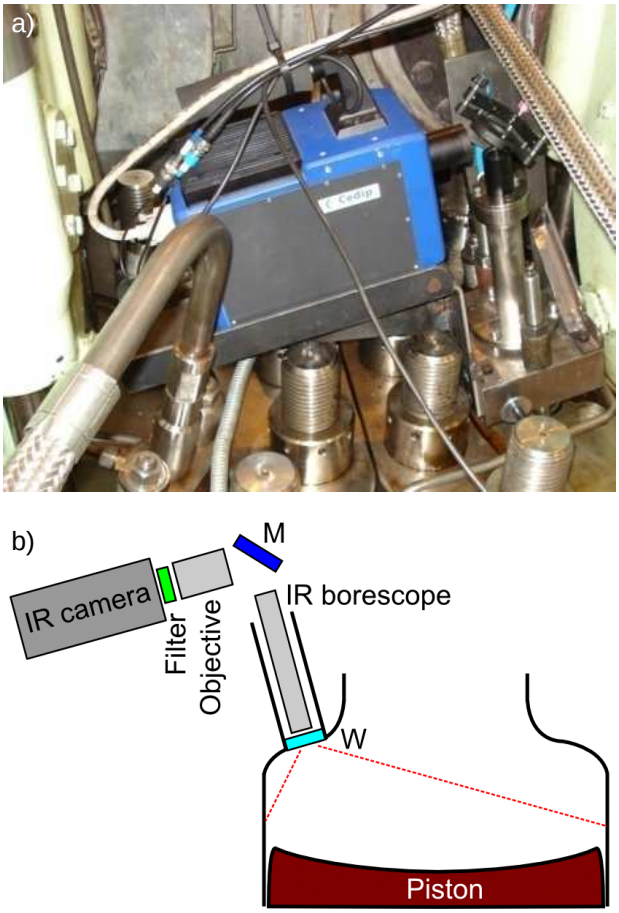

Figure 16 - a) Photo of IR camera mounted on engine, b) schematic illustration of imaging arrangement.

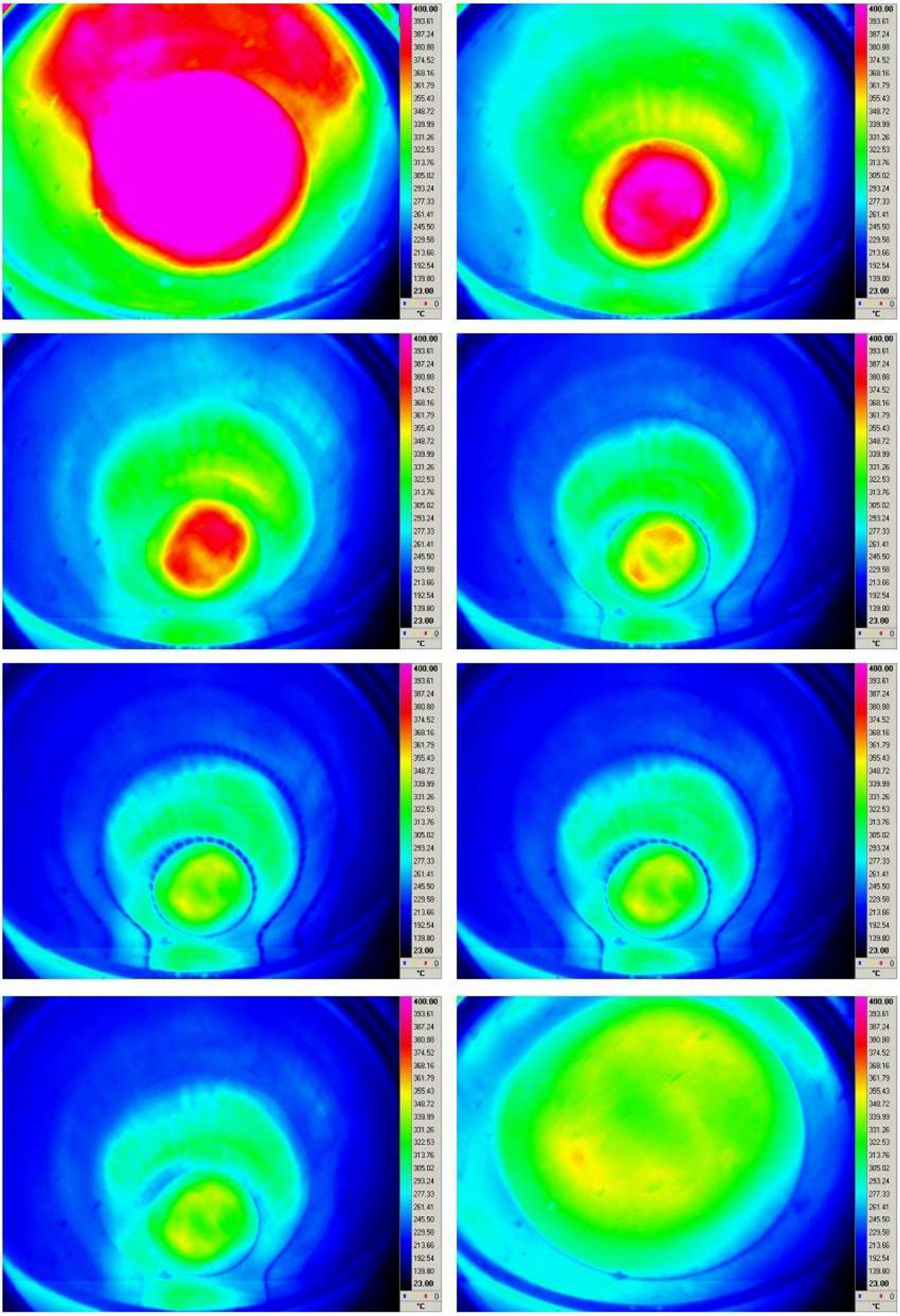

Figure 17 - Piston surface temperatures over a single-cycle, measured using an IR-camera fitted with a 3.9 μm optical filter, during 50% engine load.

Results

For thermometry the IR-camera, mounted on its frame with bending mirror, endoscope optics and sapphire window in place was calibrated before and after measurements with a portable blackbody at 300°C. The IR-camera is very sensitive to changes in temperature of the camera itself, and a drift in background signal was observed during the experiments. Therefore an increased uncertainty must be ascribed to absolute temperature values. The surface of the piston is covered by a layer of deposits containing soot and the emissivity of the surface is expected to be very high, around or larger than 0.95. In the following the emissivity is set to 1.00 for simplicity, thus giving slightly lower surface temperatures than with an emissivity 0.95. A certain thickness of this layer might result in very high surface temperatures in periods with strong thermal heat radiation from the gas and soot, due to reduced heat transfer by conduction by the insulating layer to the underlying piston material. An example of eight temperature images recorded during a single engine cycle is shown in Figure 17. The same colour scale, which ranges from 23°C to 400°C, is used in all images. Due to the off-centre viewing angle a slightly skewed view of the cylinder interior is obtained. In frame 5, close to BDC, the uncovered scavenge port at the bottom of the cylinder are seen. At the steep angle of observation used the liner wall material is highly reflective, and temperatures can thus not be deduced from this region, but only from the piston surface. The signal at the liner wall thus comes from multiple reflections of the thermal radiation from the bottom of the cylinder, and one can even see several sets of reflections from the scavenging ports, e.g. in frame 5.

As expected the piston temperature is seen to be highest after combustion, and then cools down during scavenging. An asymmetric temperature distribution is observed, which reflects the pattern of radiative loading from the two flames, and also from the uneven inflow of cold air through the scavenging ports. A rapid cooling by more than 50° at the edge of the piston, once the scavenging ports are uncovered, can be seen (frame 4-5).

By using band-pass filters in the spectral region where either CO_2 or H_2O vapour is emitting/absorbing heat radiation the high temperature exhaust gas during the scavenging can be visualized. Since the combustion chamber walls also emit some thermal radiation within that band, recordings obtained without combustion were subtracted in order to suppress this wall radiation. In Figure 18 a series of consecutive post-processed images recorded at a resolution of 11 CAD within a single cycle are shown. One can see the hot CO_2 being flushed out of the cylinder. In the latter part of the process a swirling “tornado like” pillar of hot gas is clearly seen. Two different cycles recorded under identical conditions are shown, from which a certain cycle-to-cycle variation in the structure of the hot gases can be observed.

CONCLUSIONS

A novel optical cover for the two-stroke marine test engine at MAN Diesel&Turbo in Copenhagen has been designed. It allows for flexible optical access to the top part of the combustion chamber, both for laser illumination and image capture. Here we have presented the novel capabilities offered by this system, illustrated through a series of optical measurements. Examples include detailed imaging of fuel jet structure, development and ignition; measurements of in-cylinder flow fields in order to characterize swirl as well as scavenging; and cycle resolved IR-imaging of piston temperature distributions and scavenging of hot combustion gases.

The motivation for investing in such optical capabilities is twofold. Firstly, the results will be used for advancing the predictive capabilities of numerical CFD tools - which are used extensively in engine development. The optical data can be used to establish boundary values for computations, for validating results, and also for highlighting specific

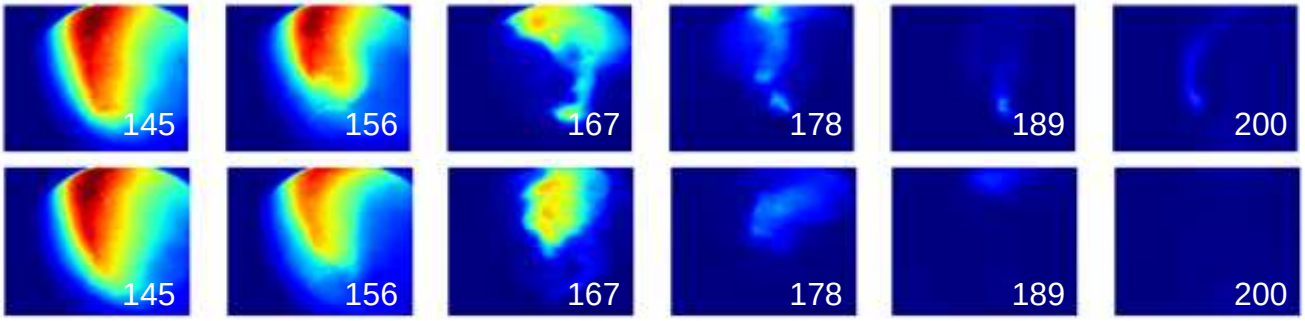

Figure 18 – Sequences of hot CO_2 emission images captured using an IR camera fitted with a 4.5 µm filter. Two different cycles are shown. The view is similar to that in Fig 17, numbers indicate CAD ATDC.

shortcomings of models. Here we have tried to present the first steps taken towards integrating the optical diagnostics with the development of computational tools. Secondly, the optical imaging methods constitute a powerful engineering tool for product development – as in cylinder phenomena such as fuel jet penetration, flame ignition and structure, and thermal loads can be visualized in real time.

Based on the success of the first measurement campaigns executed on the optical cover we plan to pursue this line of research. As well as adapting new measurement techniques for studies of other relevant engine properties and phenomena, we also plan to employ the same techniques demonstrated here to further explore other engine operating regimes or modes, thus extending our experimental data base further. Concurrently, efforts will also be devoted to data post-processing and development of methods for comparisons of experimental and computational results, in order to advance the predictive capabilities of the latter.

ACKNOWLEDGEMENTS

The research leading to these results has received funding from the European Union Seventh Framework Programme FP7/2007-2013 under grant agreements n° 217878 (HerculesB) and 284354 (HerculesC). We would like to thank Mark Hoffmann (MAN Disel&Turbo SE) for engine cycle simulations of exhaust valve flows.

REFERENCES

[1] DEC J.E. “A conceptual model of DI diesel combustion based on laser-sheet imaging” SAE technical paper (970873), 1997.

[2] DEC J.E. “Advanced compression-ignition engines – understanding the in-cylinder processes” Proc. Combust. Inst., Vol. 32, 2009, pp. 2727-2742.

[3] KOHSE-HÖINGHAUS K. and JEFFRIES J.B. (Eds.) “Applied Combustion Diagnostics” Taylor & Francis, New York, 2002.

[4] SCHULZ C. and SICK V. “Tracer-LIF diagnostics: quantitative measurement of fuel concentration, temperature and fuel/air ratio in practical combustion systems” Prog. Energy Combust. Sci., Vol. 31, 2005, pp. 75-121.

[5] WINKELHOFER E., FUCHS H., and MOROZOV A. “Lasers in chemistry vol 1, ed M Lackner” Wiley-VCH, Weinheim, 2008, pp. 503-530.

[6] WALDENMAIER U., METZGER J., PORTEN P., STIECH G., HEIDENREICH T., and WAGNER U. “Optical and numerical investigations of the combustion process in a single cylinder medium speed diesel engine” CIMAC Congress, 2010, paper nbr. 247.

[7] VATTULAINEN J., NUMMELA V., HERNBERG R., and KYTÖLÄ J. “A system for quantitative imaging diagnostics and its application to pyrometric in-cylinder flame-temperature measurements in large diesel engines” Meas. Sci. Technol., Vol. 11, 2000, pp. 103-119.

[8] SARJOVAARA T., HILLAMO H., LARMI M., and OLENIUS T. “Optical in-cylinder measurements of a large-bore medium-speed diesel engine” SAE technical paper (2008-01-2477), 2008.

[9] KAARIO O., TILLI A., HILLAMO H., SARJOVAARA T., VUORINEN V., and LARMI M. “Liquid spray data from an optical medium-speed diesel engine and its comparison with CFD” SAE technical paper (2009-01-2676), 2009.

[10] UNFUG F., BECK K., PFEIL J., WAGNER U., WALDEMNAIER U., METZGER J., PORTEN P., and STIECH G. “Optical and numerical investigation of spray formation and flame luminosity in a single cylinder medium speed diesel engine” Proc. of JSAE Annual Conf., aper nbr. 239-20115227, 2011.

[11] UNFUG F., WAGNER U., BECK K., PFEIL J., WALDEMAIER U., CELIC O., JAESCHKE J., and METZGER J. “Investigation of fuel spray propagation, combustion and soot formation/oxidation in a single cylinder medium speed diesel engine” Proc. of ASME ICEF2012, paper nbr. ICEF2012-92038, 2012.

[12] HERRMANN K., SCHULZ R., and WEISSER G. “Development of a reference experiment for large diesel engine combustion system optimization” CIMAC Congress., 2010, paper nbr. 98.

[13] SCHULZ R., HERRMANN K., VON ROTZ B., HENSEL S., SELING F., WEISSER G., WRIGHT Y.M., BOLLA M., and BOULOUCHOS K. “Assessing the performance of spray and combustion simulation tools against reference data obtained in a spray combustion chamber

representative of large two-stroke diesel engine combustion systems" CIMAC Congress, 2010, paper nbr. 247.

[14] VON ROTZ B., HERRMANN K., WEISSER G., CATTIN M., BOLLA M., and BOULOUCHOS K. "Impact of evaporation, swirl and fuel quality on the characteristics of sprays typical of large 2-stroke marine diesel engine combustion systems" Proc. of ILASS – Europe 2011, 2011.

[15] IMHOF D. and TAKASAKI K. "Visual combustion research using the rapid compression expansion machine" MTZ industrial, Vol. 2, 2012, pp. 28-39.

[16] MAYER S., POULSEN H.H., and HULT J. "In-situ optical combustion diagnostics on a large two-stroke marine diesel engine" CIMAC Congress, 2010, paper nbr. 40.

[17] NABER J.D. and SIEBERS D.L. "Effects of gas density and vaporization on penetration and dispersion of diesel sprays" SAE technical paper (960034), 1996.

[18] AMSDEN A.A. "KIVA-3V: A Block-Structured KIVA Program for Engines with Vertical or Canted Valves" Los Alamos National Laboratory, Los Alamos, New Mexico, 1997

[19] KONG, S-C., HAN, Z., and REITZ, R.D., "The Development and Application of a Diesel Ignition and Combustion Model for Multidimensional Engine Simulations" SAE Technical Paper (950278), 1995.

[20] HAN, Z. and REITZ, R.D., "Turbulence Modeling of Internal Combustion Engines Using RNG k-e Models" Combust. Sci. and Tech., Vol. 106, 1995, pp. 267-295.

[21] HULT J. and MAYER S. "Adjustable focus laser sheet module for generating constant maximum width sheets for use in optical flow diagnostics" Meas. Sci. Technol., Vol. 22, 2011, pp. 115305.

[22] RAFFEL M., WILLERT C.E., WERELEY S.T., and KOMPENHAUS J. "Particle Image Velocimetry—A Practical Guide 2nd edn." Springer, Berlin, 2007.